Experiments in Fluids 21 (1996) 417–426 © Springer-Verlag 1996

Control of turbulent separated flow over a backward-facing step by local forcing

K. B. Chun, H. J. Sung

Abstract An experimental study was made of the flow over a backward-facing step. Excitations were given to separated flow by means of a sinusoidally oscillating jet issuing from a thin slit near the separation line. The Reynolds number based on the step height (H) varied $13\,000 \leqslant Re_H \leqslant 33\,000$. Effect of local forcing on the flow structure was scrutinized by altering the forcing amplitude ($0 \leqslant A_0 \leqslant 0.07$) and forcing frequency ($0 \leqslant St_H \leqslant 5.0$). Small localized forcing near the separation edge enhanced the shear-layer growth rate and produced a large roll-up vortex at the separation edge. A large vortex in the shear layer gave rise to a higher rate of entrainment, which lead to a reduction in reattachment length as compared to the unforced flow. The normalized minimum reattachment length $(x_r)_{\min}/x_{r0}$ was obtained at $St_\theta \cong 0.01$. The most effective forcing frequency was found to be comparable to the shedding frequency of the separated shear layer.

List of symbols

A_0	forcing amplitude $= (Q_{\text{forced}} - Q_{\text{unforced}})/U_0$
AR	aspect ratio $= W/H$
C_p	wall-pressure coefficient $= (P - P_0)/(1/2)\rho U_0^2$
ER	expansion ratio $= (2H + H)/2H$
f_f	forcing frequency, Hz
f_s	shedding frequency, Hz
g	slit width $= 1.0 \pm 0.1$ mm
H	step height $= 50$ mm
P	wall-static pressure, Pa
P_0	wall-static pressure at $x/H = -2.0$, Pa
Q_{forced}	total velocity measured at reference position for forced flow, m/s
Q_{unforced}	total velocity measured at reference position for unforced flow, m/s
Re_H	Reynolds number based on H and U_0, $= U_0 H/\nu$
St_H	Reduced forcing frequency, Strouhal number $= f_f H/U_0$
St_θ	Reduced forcing frequency based on the momentum thickness $= f_f \theta/U_0$
U, V	streamwise and vertical time-mean velocity, m/s
u	streamwise fluctuation velocity, m/s
U_0	free-stream velocity, m/s
$\sqrt{\overline{u^2}}$	r.m.s. intensity of streamwise velocity fluctuation, m/s
x_r	reattachment length, m
x_{r0}	reattachment length for $A_0 = 0$, m
x, y, z	distance of streamwise, vertical and spanwise respectively, m
W	width of test section $= 625$ mm

Greek symbols

δ	boundary-layer thickness, cm
δ^*	displacement thickness, cm
γ_p	forward-flow time fraction
ρ	density of air for measurement, kg/m^3
ν	kinematic viscosity of air for measurement, m^2/s
θ	momentum thickness, cm

1 Introduction

Typical flow patterns over a backward-facing step at high Reynolds numbers display formation of separated flow near the separation edge as well as the emergence of reattached flow downstream. The presence of a separated flow, together with a reattaching flow, gives rise to increased unsteadiness, pressure fluctuations, structure vibrations and noise. It is necessary to understand the physics of the phenomenon and to find possible methods to ameliorate the above-mentioned adverse impacts.

A literature survey reveals that there have been many attempts to control or lessen the unfavorable behavior associated with separated and reattaching flows. The method of an oscillating sharp separation edge was proposed by Roos and Kegelman (1987). Use of sound waves to influence the reattachment process was examined by several researchers (Bhattacharjee et al. 1986; Cooper et al. 1986; Zaman et al. 1987; Nishioka et al. 1990 and others). In particular, introduction of a local forcing in the vicinity of the separation edge has been contemplated (Kiya et al. 1993; Sigurdson 1995). These experimental efforts utilized a small-amplitude localized jet flow close to the square-cut leading-edge of a blunt body. The jet flow contained a well defined single-frequency pulsation. Frequency and amplitude of this pulsating jet were varied in experiments for a blunt-based circular cylinder (Kiya et al. 1993; Sigurdson 1995). It was demonstrated that, by means of small localized perturbation near the separation edge, overall characteristics of the separated and reattaching flows were altered significantly.

Received: 29 November 1995/Accepted: 10 May 1996

K. B. Chun, H. J. Sung
Department of Mechanical Engineering
Korea Advanced Institute of Science and Technology
373-1 Kusong-dong, Yusong-ku, Taejon, 305–701, Korea

Correspondence to: H. J. Sung

The afore-said method of controlling the separated and reattaching flow presents a promising ground for further study. The idea is that unfavorable characteristics may be reduced by the introduction of a small, localized perturbation near the vicinity of the separation edge. The success of the prior experiments suggests a need to extend experimental studies into the feasibility of separation control. In view of the relatively simple configuration, turbulent flow over a backward-facing step was selected for further experimental study. The local forcing was produced by a single-frequency sinusoidal disturbance at the separation edge through a thin slit. The principal rationale for selecting this flow configuration was that this flow is frequently used as a benchmark problem for separated and reattaching flows. If the local forcing mechanism is found to be effective for controlling the separated and reattaching flows, then the possibilities of the present control mechanism for other types of turbulent flows would be high.

It is known that large-scale vortical structures are essential ingredients in separated and reattaching shear flows. Although the process of large-scale vortex development has been investigated extensively in unbounded flows such as jets and wakes, little information was available for bounded flows. The main objective of the present efforts is to delineate the salient characteristics of large-scale vortex development in bounded flows, where the flow is excited by a sinusoidal oscillating jet issuing from a separation line. Clearly, prominent flow characteristics of separated shear flow can be studied by varying the local forcing frequency and amplitude. The present aim is to acquire more comprehensive and systematic flow data by local forcing over broader ranges of the frequency and amplitude.

In the experimental setup, step height was fixed at $H = 50$ mm and the expansion ratio ER, was equal to 1.5. The Reynolds number based on the step height (H) varied from $13\,000 \leqslant Re_H \leqslant 33\,000$. The pulsation frequency varied from $25\ \text{Hz} \leqslant f_f \leqslant 5\ \text{kHz}$. Special attention was given to the definition of the forcing amplitude ($0.03 \leqslant A_0 \leqslant 0.07$). By changing the frequency and amplitude, the response of the separated and reattaching flow was analyzed in terms of the reattachment length, static-wall pressure, mean velocity, turbulent quantities and relevant dynamic spectra. It was found that the local forcing enhanced the coherence of the separated shear layer and reduced the reattachment length. The reattachment length was shown to attain a minimum at a particular forcing frequency. These experimental data provide baseline source from which numerical model prediction for flow control could be compared.

2 Experimental apparatus and procedure

2.1 Wind tunnel

A subsonic open-circuit wind tunnel was constructed for the present experiment. The settling chamber, honeycomb and screens were placed in sequence. Smooth contraction fairing with a large contraction ratio (6 : 1) and flow conditioning elements (honeycomb and three screens) in the settling chamber ensured a high-quality flow in the test section. The free-stream turbulence intensity was less than 0.6% at speeds 4.0 to 14.0 m/s. No significant peaks were found in the spectrum of velocity fluctuations in the main flow. The dimensions of the inlet channel were: the spanwise width $W = 625$ mm, height $2H = 100$ mm, and the length in the streamwise direction was 750 mm. A trip wire was installed at the entrance of the inlet channel to make the inlet flow uniformly turbulent. Figure 1 shows a schematic view of the configuration of the test section. The step height (H) of a backward-facing step was 50 mm and the aspect ratio AR, was equal to 12.5. For the present experimental setup, the two-dimensional flow assumption was applicable to reasonable accuracy for much of the central portion of the test section (de Brederode and Bradshaw 1978). The extent of two-dimensionality of forced flows is shown in Fig. 2.

A 30 cm woofer acoustic speaker was mounted inside the chamber. The woofer was driven by a power amplifier and

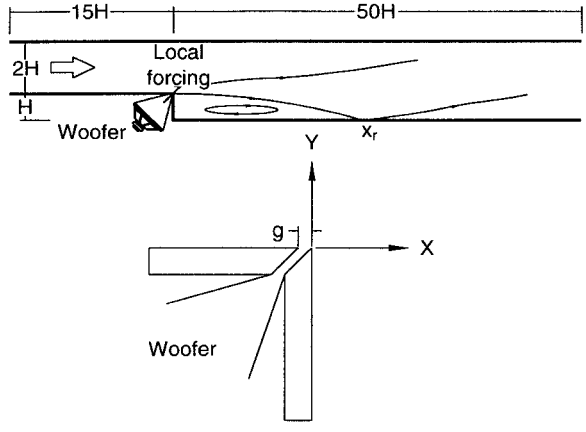

Fig. 1. Schematic diagram of wind tunnel and relevant coordinates

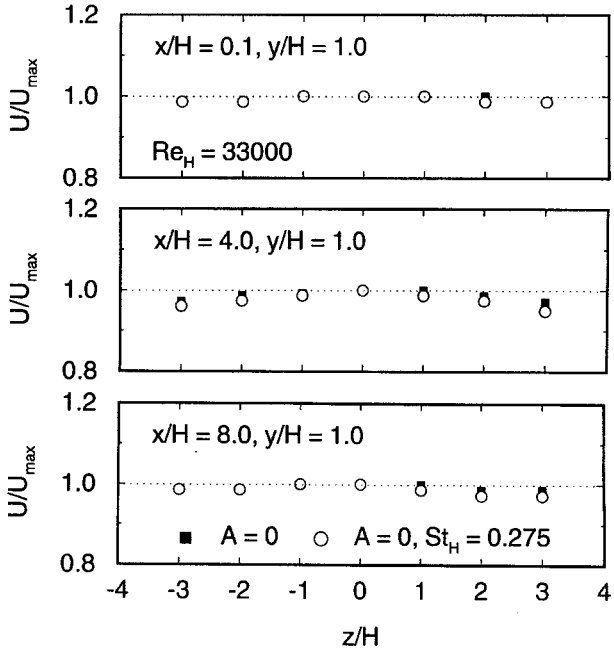

Fig. 2. Extent of two-dimensionality for $Re_H = 33\,000$

a signal generator with a sinusoidal output of controllable frequency and amplitude. A sinusoidal velocity fluctuation was introduced through a spanwise thin slit along the separation line. The width of the slit g, was equal to 1.0 ± 0.1 mm. As illustrated in Fig. 1, the origin of the x, y coordinates was located at a position on the separation point.

2.2 Local forcing

The forcing technique was produced by emitting acoustic sinusoidal oscillation waves from the speaker, located inside the chamber. The wave reached the flow through a small gap located at the separation edge, which allowed the velocity fluctuation, due to the waves, to be superimposed on the external flow. The definition of the forcing amplitude should be made in the presence of the main flow in the wind tunnel. This is because pressure near the separation edge will interact with the main flow and is expected to be lower than in the absence of the main flow. Moreover, pressure distributions are frequency-dependent due to flow-field variations at each forcing frequency. In this way, the necessary power to drive the woofer was adjusted to produce a constant forcing amplitude for each local forcing frequency being tested. It was found that, at a fixed frequency, the velocity perturbation was a linearly increasing function of voltage.

The forcing amplitude (A_0) was defined as the ratio of the difference of total velocity (Q) due to oscillation to the mean free-stream velocity (U_0), $A_0 = (Q_{\text{forced}} - Q_{\text{unforced}})/U_0$. The total velocity was Q, was equal to $(U^2 + V^2)^{1/2}$, where U and V are the time-mean velocity fluctuation components in the x and y directions, respectively. The total velocity was measured at the position $(x/H, y/H) = (-0.02, 0.01)$. The present definition of A_0 is based on the momentum change between the unforced flow and the forced flow for the initial boundary layer. In the present experiment, $(Q_{\text{forced}} - Q_{\text{unforced}})$ was always less than 7% of the free-stream velocity. The experiment was carried out over extended ranges of $St_H (0 \leqslant St_H \leqslant 5.0)$ and $A_0 (0.03 \leqslant A_0 \leqslant 0.07)$ at moderate Reynolds numbers ($13\,000 \leqslant Re_H \leqslant 33\,000$). In the above, the nondimensional frequency $f_f H/U_0$, is denoted by St_H, which will be referred to as the reduced forcing frequency hereafter.

2.3 Instrumentation and data acquisition

To measure the wall-static pressure, a number of pressure taps of 1 mm diameter were installed along the bottom wall of the test section. A scannivalve (FC-091) and a micromanometer (FC-012) were connected to the taps. The pressure signal (sampling frequency 6 Hz) was connected to an IBM-486 through a A/D converter (HP3456A). A total of 4096 individual pressure signals were time-averaged to obtain a pressure coefficient for each point measured.

Standard hot-wire measurements were made using a TSI-IFA 100 constant temperature anemometer. A TSI model 1246 T1.5 cross-wire probe was used to measure the turbulent properties except in the recirculation region. A TSI model 1250 single-wire probe was employed to measure the local forcing amplitude, and a TSI model 1288 split-film probe was utilized to detect the forward-flow time fraction γ_p. To ensure precise measurement positions, probes were moved in the x and y directions by a remote controlled traverse system. The resolution was found to be within 0.025 mm. Accurate positioning of the probe was achieved by a digital height gauge with a sighting microscope, where the resolution was within 0.01 mm.

3 Results and discussion

The experiment on flow over a backward-facing step without local forcing was first performed. Prior results of experiments are available for comparison with the present results and are summarized in Table 1. In the present experiment, three Reynolds numbers were tested, i.e., $Re_H = 13\,000$, 23 000 and 33 000. In Table 1, other experimental conditions are listed. As compared with the other experimental results (Bradshaw and Wong 1972; Eaton and Johnston 1980; Kim et al. 1980), the present experimental results are in reasonable agreement with previous findings.

Among the various quantities characterizing the backward-facing step flow, the reattachment length (x_r) is frequently used as a representative quantity in a time-mean sense. In order to find the reattachment length, the forward-flow time fraction (γ_p) in the vicinity of the wall ($y/H = -0.98$) was measured by using a split-film probe (TSI model 1288). The time-mean reattachment position (x_r) was defined as the point where the forward-flow time fraction was equal to $\gamma_p = 0.5$.

Three forcing levels ($A_0 = 0.03$, 0.05 and 0.07) are chosen to testing, where the forcing amplitude A_0 was determined with wind-tunnel flow. As a measure of effectiveness of the local forcing, the normalized reattachment length x_r/x_{r0} was plotted and shown in Fig. 3. Here, x_{r0} denotes the time-mean reattachment length without local forcing, i.e., the unforced flow ($A_0 = 0$). The forcing frequency was varied over a range of $0 \leqslant St_H \leqslant 5.0$. Experiments then were repeated by varying the forcing amplitude and frequency. As emphasized earlier, the effect of local forcing on the reattachment length is substantial. At a high forcing level ($A_0 = 0.07$), the reattachment has a single minimum approximately at $St_H \cong 0.27$ as displayed in Fig. 3a.

This particular forcing frequency may be referred to as the most effective forcing frequency. As reported by Sigurdson (1995), it is expected that the most effective frequency is close to the natural vortex shedding frequency of the separated shear

Table 1. Comparison of present experiment with other experimental results

Case	Re_H	Re_θ	δ/H	AR	ER	x_r/H
Bradshaw and Wong (1972)	42 000	730	0.13	30.5	1.25	6.0
	39 000	890	0.23			7.97
Eaton and Johnston (1980)	23 000	510	0.23	12	1.667	8.20
	11 000	240	0.18			6.97
Kim et al. (1980)	30 000	1400	0.45	24	1.5	7 ± 1
	45 000	1400	0.30	16		7 ± 1
	33 000	1340	0.41			7.80
Present	23 000	890	0.38	12.5	1.5	7.20
	13 000	480	0.28			6.75

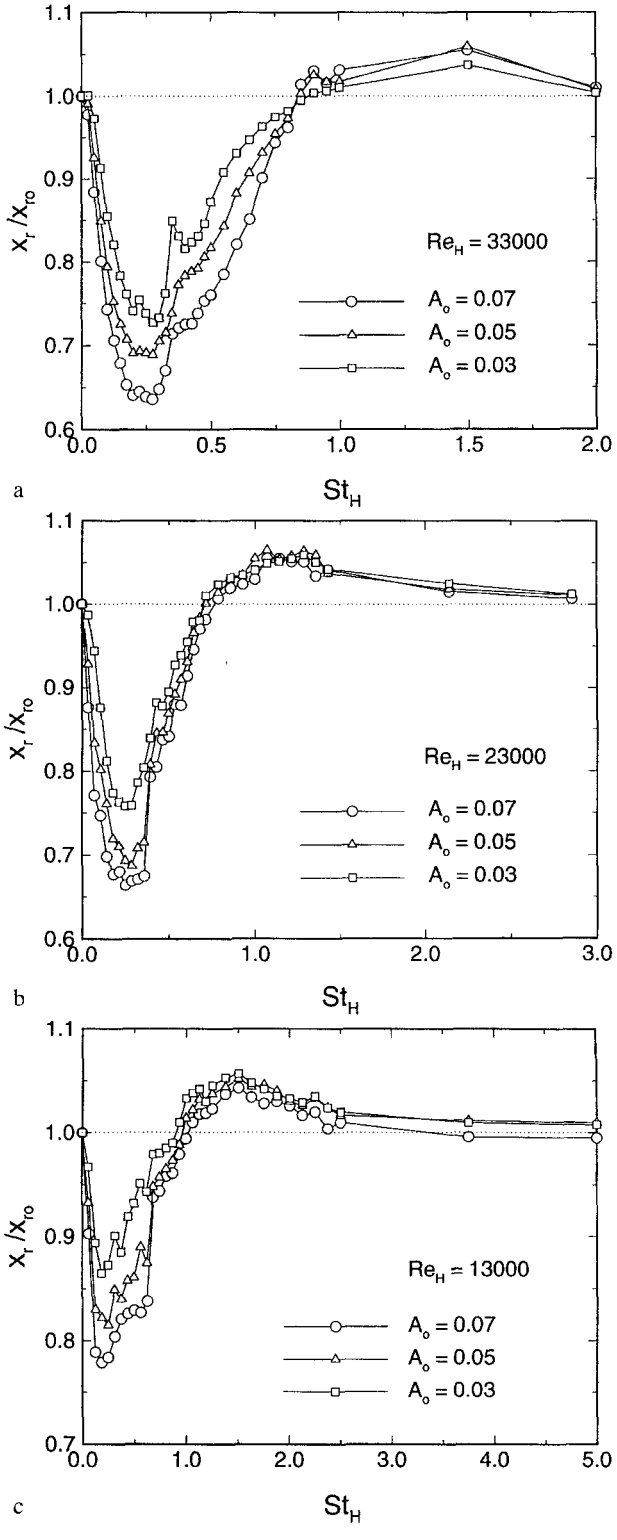

Fig. 3a–c. Normalized reattachment x_r/x_{r0} against forcing frequency St_H. **a** $Re_H = 33\,000$, **b** $Re_H = 23\,000$, **c** $Re_H = 13\,000$

layer. A global feature observed in Fig. 3a, indicates that the forcing amplitude (A_0) affects only the total size of reattachment length, i.e., the reattachment length decreases generally with increasing forcing levels.

However, a closer inspection of Fig. 3a for lower forcing amplitude ($A_0 = 0.03$) discloses that the double minima of x_r/x_{r0} are observed at about $St_H \cong 0.27$ and $St_H \cong 0.40$. These two distinct minima also have been detected by other researchers (Nagib et al. 1985; Kiya et al. 1993). The smaller reduced frequency ($St_H \cong 0.27$) is related to the shedding-type instability in the separated shear layer and is associated with the momentum exchange induced by the modulation of the separated shear layer (Nagib et al. 1985). For a large value for the reduced frequency ($St_H \cong 0.40$), the dominating mechanism is the formation and shedding of energetic vortices caused by local forcing. This effect may be related to the shear layer instability in the initial boundary layer. It is known that the local forcing increases the shear-layer growth rate and produces a large roll-up vortex at an earlier separation edge. A large vortex in the shear layer produces a higher rate of entrainment, which leads to the reduction of the reattachment length as compared to the unforced flow ($A_0 = 0$). Details regarding the role of the forcing frequency involved in vortex-merging will be discussed in the spectral analysis section.

When the forcing frequency is larger than a critical value, i.e., $St_H \geqslant 0.8$, the reattachment length is seen to be independent of the forcing frequency. Additionally, as St_H increases, the reattachment length is even larger than that of the unforced flow ($A_0 = 0$), i.e., $x_r/x_{r0} \geqslant 1$. This may be attributed to the down stream stretched vortices without vortex-merging. The maximum reattachment length, as shown in Fig. 3a, can be observed. This is in conformity with the experimental findings of Kiya et al. (1993). For two different Reynolds numbers ($Re_H = 13\,000$, $23\,000$), similar trends can be found in Fig. 3b and Fig. 3c. However, as Re_H decreases ($Re_H = 13\,000$), the region of $x_r/x_{r0} \geqslant 1$, due to local forcing is elongated.

The normalized minimum reattachment length $(x_r)_{\min}/x_{r0}$ as a function of A_0 is presented in Fig. 4 for three Reynolds numbers. This is designated to examine the effect of forcing amplitude (A_0) on the reduction of the reattachment length. As A_0 increases ($0.03 \leqslant A_0 \leqslant 0.07$), $(x_r)_{\min}/x_{r0}$ decreases linearly on a logarithmic scale. This implies that, as A_0 is further increased ($A_0 \geqslant 0.07$), the reduction rate of x_r will decay in a linear fashion. It is known that the mechanism of decreasing reattachment length is more dependent on the forcing frequency than on the forcing amplitude (Kiya et al. 1993).

The effect of initial boundary-layer conditions on the unsteady separated flows is shown in Fig. 5. Before proceeding further, it should be demonstrated that three representative forcing cases are selected in the present experiment to distinguish the flow structures by local forcing at $Re_H = 33\,000$. The first selection is the case of no forcing ($A_0 = 0$). The second is the case of $A_0 = 0.07$, $St_H = 0.275$, which yields a minimum reattachment length in Fig. 3a. The last is the case of $A_0 = 0.07$, $St_H = 1.00$, which gives an enlargement of the reattachment length, $x_r/x_{r0} \geqslant 1$. As observed in Fig. 5, no significant differences are found in the mean velocity profiles (U/U_0) for three cases near the separation edge ($x/H = -0.02$). This suggests that the strength of local forcing is relatively weak and can not significantly influence the mean velocity across the free-stream flow ($0 \leqslant y/H \leqslant 0.20$). However, the effect of local forcing on turbulence is significant at the separation edge. In particular,

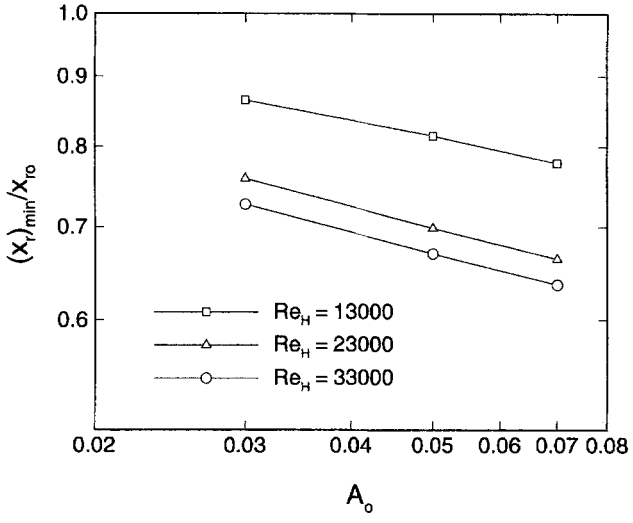

Fig. 4. Normalized minimum reattachment length $(x_r)_{min}/x_{r0}$ against forcing amplitude A_0 for three Reynolds numbers

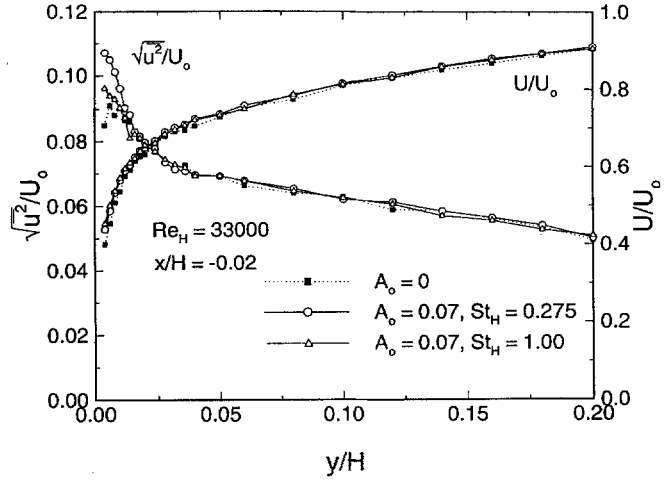

Fig. 5. Distributions of U/U_0 and $\sqrt{\overline{u^2}}/U_0$ at $x/H=-0.02$ for three forcing cases. $Re_H=33\,00$

the turbulence intensity $\sqrt{\overline{u}^2_{max}}/U_0$ is very large near the edge ($y/H=0.01$) at the local forcing $A_0=0.07$, $St_H=0.275$. The flow apparently modifies the rolling-up process of the shear layer in the vicinity of the sharp separation edge. This disturbance is convected downstream, which causes large increases in entrainment close to the separation edge. The increased entrainment causes the time-averaged streamlines to have a small radius of curvature near the separation edge.

The reduced reattachment length is closely related to the increased growth rate of the shear layer and the curvature toward the wall. It is evident that the growth rate depends on how well the shear layer is forced (Battacharjee et al. 1986). Among the initial boundary-layer parameters, the adoption of the momentum thickness (θ) near the separation edge is more useful in the discussion of the similarity of the reduced reattachment length than that of the step height (H). Based

Table 2. Initial boundary layer conditions at $x/H=-0.02$

Re_H	Forcing condition	δ	δ^*	θ	δ^*/θ
33 000	$A=0$	20.60	2.62	2.03	1.29
	$A=0.07$, $St_H=0.275$	17.65	2.49	1.96	1.27
	$A=0.07$, $St_H=1.0$	21.05	2.48	1.94	1.28
23 000	$A=0$	19.12	2.51	1.86	1.35
	$A=0.07$, $St_H=0.286$	16.94	2.43	1.82	1.33
	$A=0.07$, $St_H=1.286$	17.01	2.42	1.81	1.34
13 000	$A=0$	14.21	3.71	1.82	2.04
	$A=0.07$, $St_H=0.25$	14.50	3.59	1.78	2.02
	$A=0.07$, $St_H=1.50$	14.33	3.74	1.79	2.09

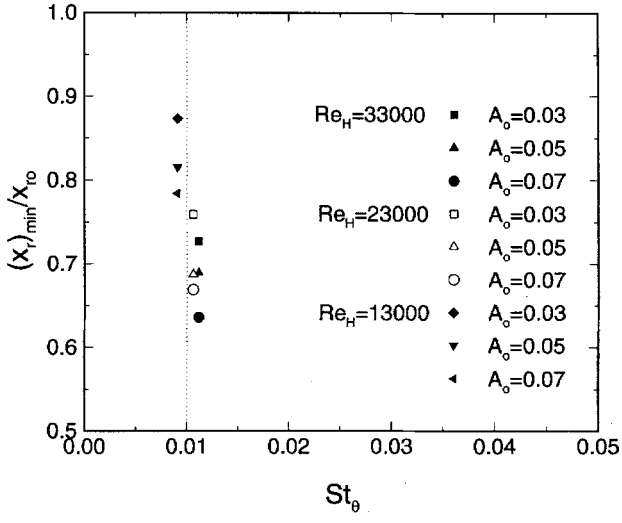

Fig. 6. Normalized minimum reattachment length $(x_r)_{min}/x_{r0}$ against St_θ

on the momentum thickness (θ), a different version of the reduced forcing frequency can be defined as $St_\theta=f_f\theta/U_0$. The normalized minimum reattachment length $(x_r)_{min}/x_{r0}$ is presented as a function of St_θ in Fig. 6 for three Reynolds numbers. In contrast to the case of St_H (Fig. 4), the effective reduced forcing frequency was obtained at $St_\theta \cong 0.01$, while a slight deviation is found at $Re_H=13\,000$. This result is generally consistent with other experimental findings (Eaton and Johnston 1980; Zaman and Hussain 1980; Battacharjee et al. 1986; Hasan 1992; Kiya et al. 1993), which are summarized in Table 3.

The measured distributions of the forward-flow time fraction γ_p on the surface near the bottom wall ($y/H=-0.98$) are represented in Fig. 7. The point of $\gamma_p=0.5$ corresponds to the reattachment position (x_r). It is shown that the reattachment length ($x_r=5.0$) of the forced flow of $A_0=0.07$ and $St_H=0.275$ is much shorter than that ($x_r=7.8$) of the unforced flow. For the unforced flow ($A_0=0$), a separation point ($\gamma_p=0.5$) is seen near the corner ($x/H=1.0$). This suggests the existence of a secondary recirculation near the corner section, which has been reported in other experimental findings (Eaton and Johnston 1980). However, for the forced flows, no secondary flows are detected near the corner region.

Table 3. The most effective reduced frequency on the shear layer

Case	Re_H	θ	St_H	St_θ
Bhatacharjee et al. (1986)	26 000	1.01	0.35	0.007
Hasan (1992)	11 000	0.68	0.55	0.012
Kiya et al. (1993)	12 0000	0.015	1.6	0.012
Eaton and Johnston (1980)	39 000	1.22	0.65	0.013
Zaman and Hussain (1980)	32 000 ~ 12 0000		0.85	0.012 ~ 0.017
Present	33 000	1.96	0.275	0.011
	23 000	1.82	0.286	0.010
	13 000	1.78	0.25	0.009

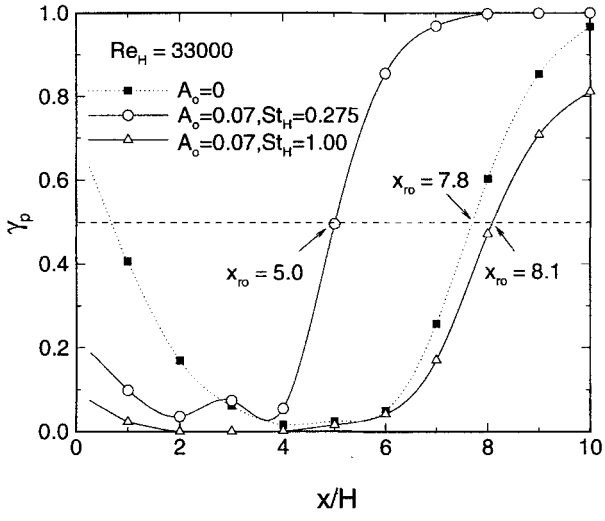

Fig. 7. Distributions of the forward-flow time fraction γ_p for three forcing cases. $Re_H = 33\,000$

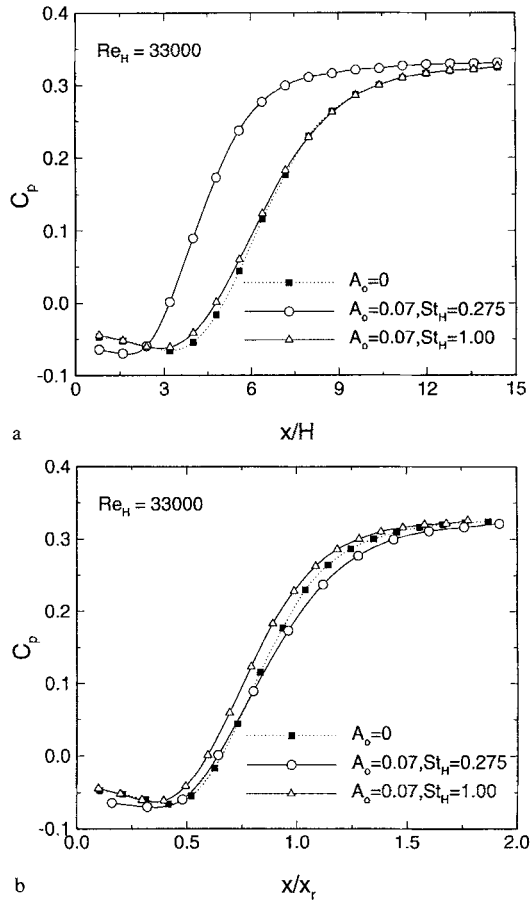

Fig. 8. a Distributions of wall pressure coefficient C_p against x/H for three forcing cases $Re_H = 33\,000$, b distributions of wall pressure coefficient C_p against x/x_r for three forcing cases. $Re_H = 33\,000$

The effect of local forcings on the mean static pressure distribution (C_p) is shown in Fig. 8a. The static pressure coefficient is defined as $C_p = (P - P_0)/(\frac{1}{2}\rho U_0^2)$, where P_0 and U_0 respectively denote the reference values of the static pressure and streamwise mean velocity at $x/H = -2.0$. The influence of local forcing on C_p is profound for $A_0 = 0.07$ and $St_H = 0.275$. The region of low-pressure level is relatively small and zero-crossing of C_p is located in the neighborhood of $x/H = 3.0$. A rapid increase of C_p is displayed, i.e. the beginning of the pressure recovery area is abruptly moved upstream. This gives rise to a substantial reduction of the reattachment length. For other two cases ($A_0 = 0$ and $A_0 = 0.07$, $St_H = 1.00$), the pressure recovery curves behave in a self-similar fashion. Low values of C_p are observed in a large region, i.e. $x/H = 5.0$. After sustaining a wide range of low pressure level, a slight increase of the pressure coefficient is exhibited. No significant difference between the two cases is seen in the overall shapes of C_p. This indicates that the pressure coefficient alone is not sufficient to characterize the entire flow mode. The general feature of C_p for $A_0 = 0$ is qualitatively consistent with the other published results (Gai and Sharma 1987). The nondimensional distance x_r/x_{r0} is adopted as the abscissa to drive a self-similarity. As shown in Fig. 8b, the corresponding pressure recovery curves for three cases appear to reach a self-similarity state.

To document the effect of local forcing on the time-averaged flow, a detailed measurement was performed at $Re_H = 33\,000$ for three local forcings. As shown in Fig. 9a, a relatively large effect by local forcing is displayed on the development of the separated flow. In the near-region of separation ($x/H = 1.0$), the mean velocity profiles were only slightly affected by the local forcing. However, significant changes in the mean velocity levels within the shear layer region were measured. The mean velocity levels of the local forcing ($A_0 = 0.07$, $St_H = 0.275$) were increased over those of the unforced flows ($A_0 = 0$), which suggests an increased transfer rate of the forced flow into the recirculation region. Since local forcing promotes vortex pairing, this results in shortening of the reattachment length. After reattachment ($x/H \geqslant 7.0$), the flow is gradually reestablished. However, the mean velocity changes by the local forcing ($A_0 = 0.07$, $St_H = 1.00$) were found to be insignificant before reattachment. After reattachment, a slow redevelopment is shown in Fig. 9a.

The effect of local forcing on the time-averaged turbulent energy levels is shown in Fig. 9b. The fluctuating energy levels

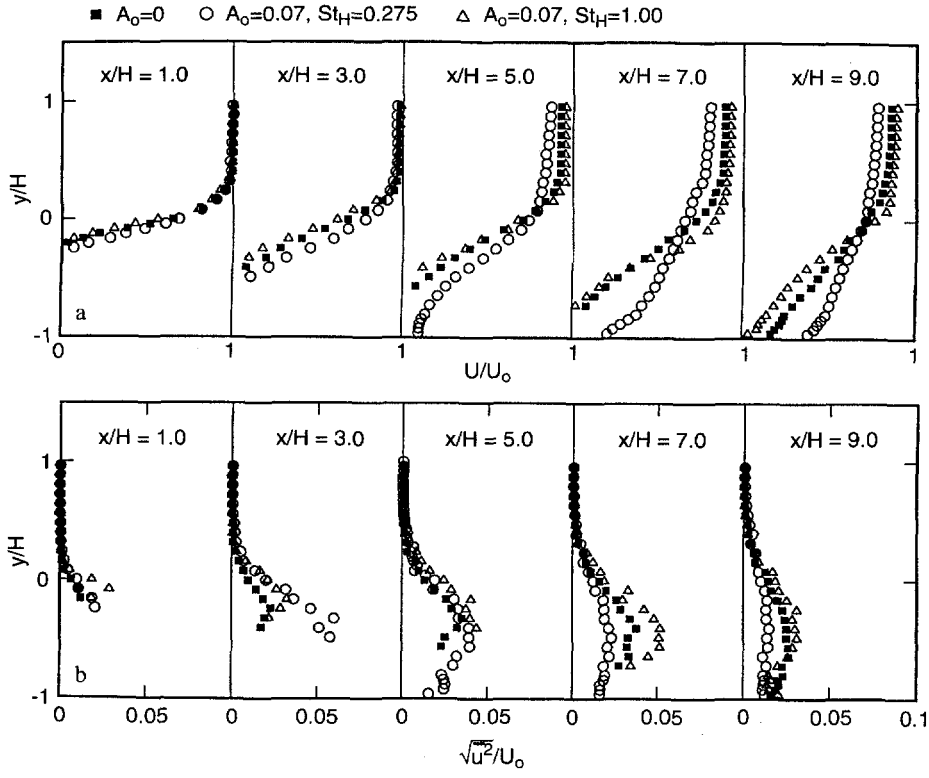

Fig. 9. Profiles of U/U_0 and $\sqrt{\overline{u^2}}/U_0$ for three forcing cases. $Re_H = 33\,000$

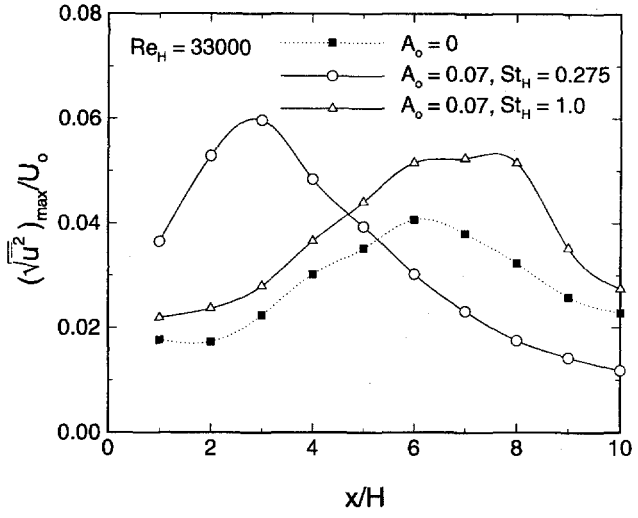

Fig. 10. Location of points of maximum turbulence level for three forcing cases. $Re_H = 33\,000$

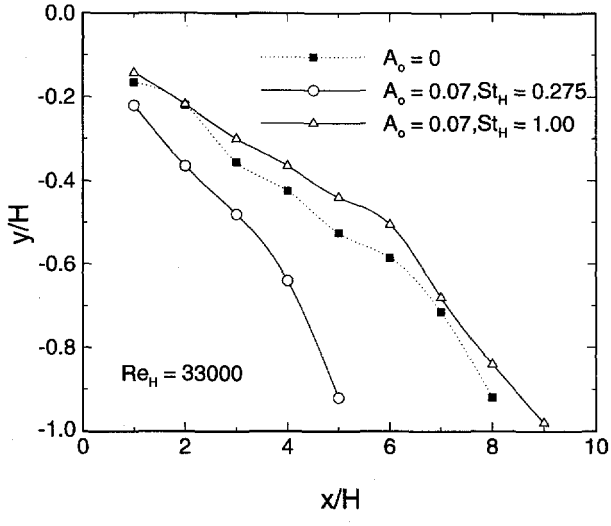

Fig. 11. Location of points of 10% free-stream velocity for three forcing cases. $Re_H = 33\,000$

are affected only slightly by the forcing near the step edge ($x/H = 1.0$), where vortices are just formed. However, the influence of local forcing on the turbulent energy levels was pronounced. In particular, the increase of turbulent energy levels by the local forcing ($A_0 = 0.07$, $St_H = 0.07$) was dominant at $x/H = 3.0$. This suggests that the amalgamation of the rolled-up vortices induced via local forcing can increase turbulence intensity levels. Accordingly, the maximum turbulence intensity is much higher than that of the unforced flow. Downstream of $x/H = 5.0$, the changes in the turbulent energy levels created by the local forcing are observed to decrease. These decreases continue until the influence on the turbulent energy levels becomes relatively small which occurs far downstream of reattachment ($x/H = 9.0$).

The locus of maximum streamwise turbulence intensity $(\sqrt{\overline{u^2}})_{max}/U_0$ is presented in Fig. 10. It can be seen that the maximum turbulence level for $A_0 = 0$ continues to increase until reattachment and then decreases afterward. In the case of $A_0 = 0.07$, $St_H = 0.275$, the maximum level increases rapidly, reaching a maximum near $x/H = 3.0$, and then subsequently decreases. It is thought that strong enhancement of the rolled-up vortices by the forcing contributes to the increase of

turbulence levels in the recirculating region. However, in the case of $A_0 = 0.07$, $St_H = 1.0$, the maximum turbulence level increases slowly and decreases at a faster rate. This implies that the flow structure in the redeveloping region has recovered to an equilibrium state (Bradshaw and Wong 1972). The overall turbulence levels for $A_0 = 0.07$ and $St_H = 1.0$ are higher than those of $A_0 = 0$. No appreciable differences were observed in the wall-static-pressure coefficient in Fig. 8a.

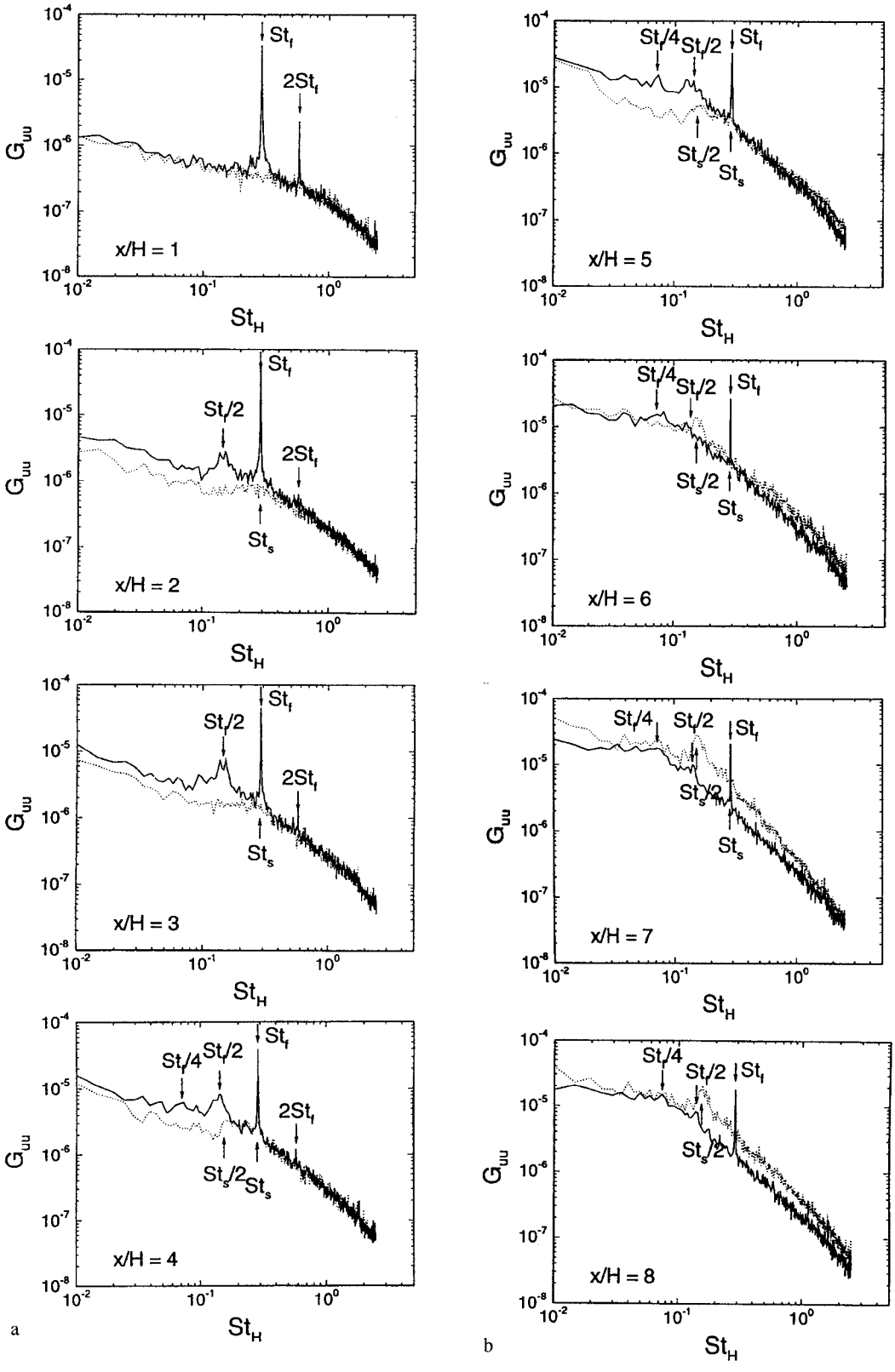

Fig. 12a, b. Velocity spectra along the streamwise position. $A = 0$ (dotted line), $A = 0.07$ and $St_H = 0.275$ (solid line)

The locations of the 10% free-stream velocity are presented in Fig. 11 as a function of the downstream position. At $x/H=1.0$, the free-stream velocities are nearly the same. However, as the flow evolves downstream, the rate of shear-layer growth are dramatically changed. The curvature toward the wall is closely connected with the shrinkage of the reattachment length apparently due to an increase in entrainment. It is seen that the growth rate for $A_0=0.07$ and $St_H=0.275$ is much larger than for other cases ($A_0=0$, and $A_0=0.07$ and $St_H=1.0$). As the curve approaches the wall by extrapolation, the reattachment location can be measured asymptotically. As expected, the local forcing at $A_0=0.07$ and $St_H=0.275$ shortens the reattachment length significantly.

In an attempt to understand the mechanism of the effect of local forcing, the spectra of streamwise velocity fluctuations were measured and presented in Fig. 12 as a function of downstream distance ($1\leqslant x/H\leqslant 8$). The spectra were obtained at the position $U/U_{max}=0.95$, where the value of streamwise velocity was 95% of the maximum velocity. Comparisons are made for two cases: i) $A_0=0$, and, ii) $A_0=0.07$ and $St_H=0.275$. The spectra of $A_0=0$ are plotted with dotted lines and the spectra of $A_0=0.07$ and $St_H=0.275$ with solid lines. The notation St_f in Fig. 12 denotes the reduced forcing frequency ($St_f=f_fH/U_0$) and St_s is the reduced shedding frequency ($St_s=f_sH/U_0$). Here, the shedding frequency f_s was obtained near the reattachment position in unforced flow.

Near the separation edge ($x/H=1.0$), no significant peak is displayed for the unforced flow ($A_0=0$); whereas, a sharp peak is exhibited at the forcing frequency (St_f). It can be observed that the energy levels for both cases are relatively low. At $x/H=2.0$, a spectrum peak corresponding to the first subharmonics ($St_f/2$) of the forcing frequency begins to emerge. This suggests that a large-scale vortex amalgamation takes place in the separated shear layer apparently due to the local forcing. This vortex merging causes the increase in turbulence intensities so that the overall turbulence levels are significantly enhanced. The vortex-shedding frequency (St_s) in the unforced flow may be observed, which is nearly coincident with the present forcing frequency ($St_s\cong St_f$). This result is supportive of Sigurdson's argument that the most effective forcing frequency for minimum reattachment length is generated at or near the frequency of the shedding for unforced flow.

As the flow is convected downstream, the peak value of St_f is gradually attenuated. Conversely, the peak value of $St_f/2$ becomes larger as a function of downstream distance. At $x/H=4.0$, the second subharmonics ($St_f/4$) appears, which suggests a second vortex merging. This process results in an increase in turbulence levels. After reattachment, however, no further vortex-pairings are detected and the energy levels also are diminished. For $x/H=6.0$, the turbulence energy levels are even lower than for the case of the unforced flow. Although two vortex-pairings are present in the forced flow ($St_f/2$, $St_f/4$), only one subharmonics ($St_s/2$) appears in the unforced flow ($4.0\leqslant x/H\leqslant 8.0$). The first vortex-merging creates an increase of turbulence levels, where the turbulence levels are higher than those of the forced flow until the reattachment ($x/H=8.0$).

4 Conclusion

The effect of local forcing on flow structures over a backward-facing step have been studied experimentally, when a sinusoidal velocity fluctuation was introduced through a thin-slit near the separation line. By means of a small localized forcing effect near the separation edge, the overall characteristics of separated and reattaching flows were altered significantly. At a higher forcing level, the reattachment length had a single minimum at a specific forcing frequency. However, at lower forcing amplitudes, double minima of reattachment length were observed: i) one was related to the separated shear layer instability; and, ii) the other was attributable to the formation and shedding of energetic vortices caused by "local forcing". When the forcing frequency was greater than the critical value, the reattachment length was even larger than that of the unforced flow. It is noted that the effect of local forcing on turbulence was significant at the separation edge, where the flow tended to modify the roll-up process of the shear layer. A similarity of the normalized minimum reattachment length $(x_r)_{min}/x_{r0}$ was achieved at $St_\theta\cong 0.01$, which occurred at the reduced forcing frequency based on the momentum thickness in the vicinity of the separation edge. A rapid increase of C_p was obtained in the pressure recovery area due to the "local forcing", which gave substantial reduction of the reattachment lengths.

The effects of "local forcing" on the time-averaged flow and turbulence levels were significant. The increased mean velocity levels within the shear layer region were caused by the faster speed of the forced flow into the recirculation region. The amalgamation of the roll-up vortices increased the turbulence intensity levels. In the spectra analysis, two vortex-pairings were present in the forced flow ($St_f/2$, $St_f/4$); whereas, only one vortex-merging was observed in the unforced flow ($St_s/2$). The most effective forcing frequency for the minimum reduction of the reattachment length is close to the vortex shedding frequency of the unforced flow.

References

Bhattacharjee S; Sheelke B; Troutt TR (1986) Modifications of vortex interactions in a reattaching separated flow. AIAA J 24: 623–629

Bradshaw P; Wong FYF (1972) The reattachment and relaxation of a turbulent shear layer. J Fluid Mech 52: 113–135

de Brederode V; Bradshaw P (1978) Influence of the side walls on the turbulent center-plane boundary-layer in a squareduct. J Fluids Eng 100: 91–96

Cooper PI; Sheridan JC; Flood GJ (1986) The effects of sound on forced convection over a flat plate. Int J Heat Fluid Flow 7: 61–68

Eaton JK; Johnston JP (1980) Turbulent flow reattachment: an experimental study of the flow and structure behind a backward-facing step. Report MD-39 Thermoscience Division, Dept. of Mechanical Eng., Stanford University

Eaton JK; Johnston JP (1981) A review of research on subsonic turbulent flow reattachment. AIAA J 19: 1093–1100

Gai SL; Sharma SD (1987) Pressure distribution behind a rearward facing step. Exp Fluids 14: 154–158

Hasan MAZ (1992) The flow over a backward-facing step under controlled perturbation: laminar separation J Fluid Mech 238–73–96

Kim J; Kline SJ; Johnston JP (1980) Investigation of a reattaching turbulent shear layer: Flow over a backward-facing step. J Fluids Eng 102: 302–308

Kiya M; Shimizu M; Mochizuki O; Ido Y; Tezuka H (1993) Active forcing of an axisymmetric leading-edge turbulent separation bubble. AIAA paper 93-3245

Nagib HM; Reisenthel PH; Koga DJ (1985) On the dynamical scaling of forced unsteady separated flows. AIAA Shear Flow Control Conference: AIAA-85-0553

Nishioka M; Asai M; Yoshida S (1990) Control of flow separation by acoustic excitation. AIAA J 28: 1909–1915

Rose FW; Kegelman JT (1986) Control of coherent structures in reattaching laminar and turbulent shear layers. AIAA J 24: 1956–1963

Sigurdson LW (1995) The structure and control of a turbulent reattaching flow. J Fluid Mech 298: 139–165

Zaman KBMO; Bar-Serve A; Mangalam SM (1987) Effect of acoustic excitation on the flow over a low-Re airfoil. J Fluid Mech 182: 127–148

Zaman KBMQ; Hussain AKMF (1980) Vortex pairing on a circular jet under controlled excitation. Part 1. General jet response. J Fluid Mech 101: 449–491